Proceedings of the 2nd Marine Energy Technology Symposium
METS2014
April 15-18, 2014, Seattle, WA

ANALYSIS AND PROOF-OF-CONCEPT EXPERIMENT OF LIQUID-PISTON COMPRESSION FOR OCEAN COMPRESSED AIR ENERGY STORAGE (OCAES) SYSTEM

Joong-kyoo Park
MAE NCSU
Raleigh, NC 27695, USA

Paul I. Ro[1]
MAE NCSU
Raleigh, NC 27695, USA

Xiao He
MAE NCSU
Raleigh, NC 27695, USA

Andre P. Mazzoleni
MAE NCSU
Raleigh, NC 27695, USA

[1]Corresponding author: ro@ncsu.edu

ABSTRACT

An analysis and a proof-of-concept experiment of liquid-piston compression were conducted for a table-top Ocean Compressed Air Energy Storage (OCAES) prototype. A single-cylinder-type piston surrounded by water was modeled and analyzed based on convection heat transfer with fully developed internal flow, the assumption adopted by earlier liquid piston study in literature. Transient numerical results of this model were calculated for a polytropic compression with different polytropic index values for 2.5-second stroke. Also, an experimental model of the liquid piston was built with two different materials, polycarbonate and aluminum alloy, for a compression chamber. Temperature data were measured at six different stroke times to examine any difference in heat transfer rates affected by stroke frequency. The temperature within each cycle was measured during compression from 1 bar to 2.2 bars. It was found that longer stroke time induces smaller temperature rise in the air. The local temperature rise was observed to be 80 °C at 2.5-second stroke and 7 °C at 40-second stroke. While the simulations predict a temperature rise of 48.6 °C for a compression stroke time of 2.5 seconds, the temperature rise calculated for adiabatic compression was found to be 98.8 °C. This implies that the heat transfer characteristics of a liquid piston compression process are effective in reducing the air temperature. The experimental results with longer stroke times proved a near-isothermal nature of the liquid piston compression system. Overall, the experimental study outlined in this paper not only confirms the near-isothermal nature of the liquid piston system but also enables further study of the expansion cycle using the liquid-piston concept. More importantly, the current study paves a way for future work on a larger scale OCAES system demonstration based on liquid-piston concept.

INTRODUCTION

Energy storage systems

Renewable energy markets have grown rapidly due to the recent nuclear disaster in Japan, global warming concerns, and high fossil fuel prices. However, much of a challenge in renewable energy generation such as wind turbines, solar panel plants, and ocean-based hydrokinetic devices is related to intermittency of the sources. A real effort going forward is to maximize the usability of energy generated from these intermittent sources. Such challenge will necessitate a study on development of novel energy storage systems which would render energy from these intermittent sources more reliable and controllable.

One way of energy storage is to convert electrical energy into compressed air stored in an underground cavern. Such a system, called Compressed Air Energy Storage (CAES), has been in use for several decades. A conventional CAES system converts electrical energy into compressed air energy and stores it in a large space such as salt caverns or aquifers during low demand, and then reconverts this energy into electrical energy during high demand. The CAES system consists of three stages: compressing, storing, and expanding of air. During compression, a multi-stage

compressor with intercoolers compresses air by using electricity, while during expansion, compressed air is heated by burning of natural gas. Due to the loss of thermal energy in an underground cavern and additional heat supply required, the efficiency of the CAES system is relatively low at around 42 % [1]. In addition, other CAES drawbacks include limited maximum/minimum pressure in a cavern, pressure drops in storage due to heat losses, supplemental heating through natural gas burning during expansion cycle, and a need for a large storage space due to low efficiency, and cost of maintenance [2].

Ocean compressed air energy storage (OCAES) is first proposed by Seymour [3,4] to overcome some of the drawbacks of conventional CAES. The OCAES employs an underwater storage installed on seabed in the ocean at constant hydrostatic pressure. Also, environmental impacts and safety compromises associated with underground caverns or highly pressurized on-ground vessels are eliminated. Additionally, due to its ready scalability, one OCAES system can manage and integrate multiple intermittent offshore energy sources.

A conceptual schematic of OCAES is shown in Figure 1. On a floating or fixed platform located near renewable energy sources, multi-stage compressors and multi-stage turbines with a generator are installed. Air storage is anchored on seabed at a certain hydrostatic pressure, and air pipes are connected between the air storage and the platform to store and retrieve air. A submarine power cable is installed from the renewable energy sources to a compressor to compress air and from a generator to a power grid.

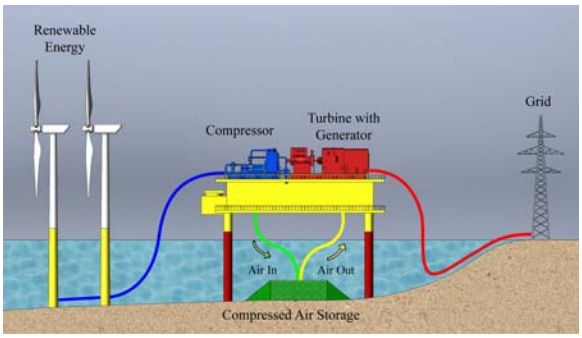

FIGURE 1. OCEAN COMPRESSED AIR ENERGY STORAGE (OCAES).

Near-isothermal process using liquid piston

Overall efficiency of OCAES system can be improved if temperature is constant or near constant during compression and expansion cycles [5]. In general, the compression and expansion of gases are regarded as adiabatic or polytropic processes, which involve a sudden increase of temperature during compression and an equally rapid decrease of temperature during expansion. Efficiency of this conventional system is much lower than an ideal isothermal process, which assumes a constant temperature of gas at all times during compression and expansion and no thermal energy loss during storage.

As a way to achieve a near-isothermal cycle, a liquid piston has been used to increase the heat transfer rate between water and air inside a reciprocating compressor and expander chamber [6-8]. During the compression phase, water and air are compressed together, and due to the high density and heat capacity of water, the temperature of water is kept at much lower threshold than the temperature of air, and the heat is transferred from air to water. Due to this heat transfer, the temperature of air increases only slightly and locally. During the expansion phase, water and air are expanded together, and the heat is transferred from water to air. Similarly, the temperature of air decreases only slightly and locally. This near-isothermal process is claimed to improve an overall efficiency over 70% [9].

ANALYSIS OF HEAT TRANSFER IN THE LIQUID PISTON

Heat transfer analysis

Figure 2 shows a simple schematic of the liquid piston for the compression and expansion cycle. The piston is initially filled with water and air as shown on the left. During compression, the incompressible water compresses the air in the piston. The heat generated by the compressed air is quickly absorbed by water and the surrounding wall of the piston. If done isothermally, the rate at which the heat transfer takes place is so rapid that the temperature remains unchanged. During expansion shown on the right, the expanded air pushes the water out. The heat lost by the expanded air is quickly recovered from water and the surrounding wall of the piston. If done isothermally, the rate at which this heat transfer in the opposite direction takes place is so rapid that the temperature remains unchanged.

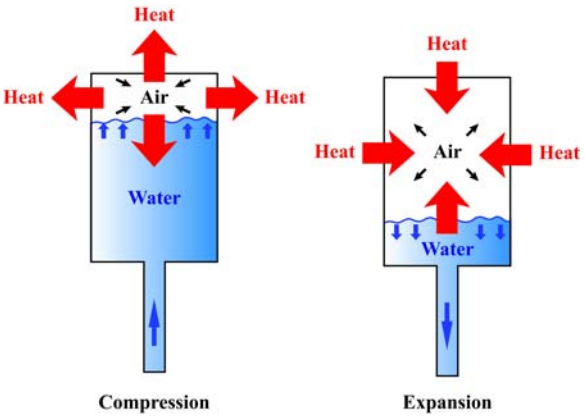

FIGURE 2. SIMPLE SCHEMATIC OF THE LIQUID PISTON SYSTEM.

In a previous study on liquid piston compression done by Van de Ven and Perry Li [10], convective heat transfer was considered as the mode of heat transfer for liquid piston compression. Since the compression chamber utilized in a table-top experimental set-up discussed later shares a similar structural shape with Van de Ven and Perry Li's model, an analytical study on temperature and pressure behavior affected by convective heat transfer in this liquid piston design was conducted. As air is compressed by water entering the chamber, convective heat transfer occurred between air and surrounding chamber wall due to increase in air temperature. The increasing temperature forces heat energy to flow from air along the chamber wall driven by the temperature difference. This flow of heat energy is defined as forced heat convection in a circular tube. Because of the unpredictable conditions caused by pressure and temperature increases and possible non-uniform fluid flow patterns inside the compression chamber, this heat transfer analysis would be very difficult to analyze. In this paper, the analysis will be simplified by assuming a fully developed internal fluid flow.

It is important to define the flow regime first when dealing with internal flows, which is determined by Reynolds number. In this case, the Reynolds number for flow in a circular tube is

$$Re_D = \frac{\rho u_m D}{\mu} \tag{1}$$

where ρ is fluid mass density, u_m is fluid mean velocity, D is the diameter of the liquid piston, and μ is fluid's dynamic viscosity. For a fully developed flow in a pipe with diameter D, experimental observations have shown that laminar flow occurs when the Reynolds number is less than 2300, while turbulent flow occurs when the Reynolds number is greater than 4000, with values in between defined as transitional flow [11]. From the initial data analysis it was found that the Reynolds number for our case did not exceed more than 650, which eliminated the necessity of including turbulent flow analysis. When analyzing heat transfer for this type of fluid flow, it is important to realize the effect of dynamic viscosity and mass density due to pressure and temperature variations. Sutherland's Equation could be used to derive dynamic viscosity of an ideal gas as a function of temperature [12]:

$$\mu = \mu_0 \frac{T_0 + C}{T + C} \left(\frac{T}{T_0}\right)^{3/2} \tag{2}$$

where μ_0 is reference dynamic viscosity, T_0 is reference temperature, T is gas temperature, and C is the Sutherland constant. Table 1 lists the Sutherland constant, reference temperature and reference dynamic viscosity for air [13,14].

TABLE 1. SUTHERLAND CONSTANTS FOR AIR.

C	$\boldsymbol{T_0}$ (K)	$\boldsymbol{\mu_0}$ (Pa-s)
120	291.15	$18.27e^{-6}$

The expression of Nusselt number needs to be determined in order to acquire convection coefficient. For fully developed laminar flow with a constant surface temperature, the Nusselt number tends to be constant [15]:

$$Nu_D = 3.66 \tag{3}$$

Knowing the expression of Nusselt number allows derivation of the convective heat transfer coefficient, h,

$$h = 3.66 \frac{k}{D} \tag{4}$$

where k is thermal conductivity of air, and its value would be evaluated at average temperature of the overall volume. For flow in a circular tube with constant density and specific heat capacity, ρ and c_p, mean temperature, T_m, could be evaluated as follow:

$$T_m = \frac{2}{u_m r_0^2} \int_0^{r_0} uTr \, dr \tag{5}$$

where r_0 is tube radius, and u is flow inlet velocity profile [16]. Then, convective heat transfer rate between air and piston wall is calculated by Newton's law of cooling:

$$q = hA_s(T_s - T_m) \quad (6)$$

where A_s is the piston inner surface area, and T_s is surface temperature. Since water is always moving up and down inside the compression chamber, both the mean temperature and the surface area are changing in time during the compression and expansion processes. Note that the same heat transfer rate can be expressed using a lumped specific heat capacity as

$$q = mc_p \frac{\Delta T_m}{\Delta t} \quad (7)$$

Then, equating the right hand sides of Equations (6) and (7), the mean air temperature change with respect to time could be expressed as

$$\frac{\Delta T_m}{\Delta t} = \frac{hA_s}{mc_p}(T_s - T_m) \quad (8)$$

This expression is useful since the variation of mean temperature is determined from the change of time or stroke frequency, which in turn facilitates a comparison of analytical data and experimental data at same stroke frequencies.

Liquid piston numerical simulations

Analytical results were generated from MATLAB. All plots shown below in Figures 3 and 4 are based on the results calculated from a polytropic compression with convective heat transfer. The desired pressure for compressed air was set to be 2.21 bars. A simplified equation used for obtaining air temperature is derived from the classic polytropic process:

$$T_2 = T_1(\frac{V_1}{V_2})^{n-1} \quad (9)$$

where n is the polytropic index. Polytropic index is an important factor in this analytical analysis in that the time at which compressed air reaches desired level varies for different polytropic indices. Furthermore, temperature change profiles were found to be highly affected by different polytropic indices. Table 2 shows the polytropic indices used for different thermal processes.

TABLE 2. POLYTROPIC INDEX RELATED TO THERMAL PROCESSES.

n=1	Isothermal process (constant temperature)
1<n<γ	Near-adiabatic process
n=γ	Adiabatic process (no heat transfer)

Here, γ is the adiabatic index and is also called heat capacity ratio. By observing the temperature profile plotted from the experimental data, the polytropic index can be estimated to see whether the compression is behaving more like an isothermal process or an adiabatic process. Finally, pressure is calculated according to the ideal gas law once the volume and temperature change were calculated by using Equations 8 and 9 as

$$P = \frac{mRT}{V} \quad (10)$$

where m is the air mass, and R is the universal gas constant. Table 3 shows the dimension of experimental chambers. For the numerical analysis, the aluminum dimension was used.

TABLE 3. DIMENSION OF LIQUID PISTON CHAMBERS.

	Polycarbonate	Aluminum
Height	6.63 in.	5.7 in.
Diameter	3.45 in.	4.7 in.
Pipe length	7 in.	7 in.
Pipe diameter	0.49 in.	0.49 in.
Volume	61.93 in.^{3}	98.89 in.^{3}

Figure 3 below is a plot of the pressure change vs. time during a 2.5-second stroke. The stroke displacement followed a sinusoidal function which was also applied to the numerical simulation performed in the next section. It is clear from the figure that the larger the polytropic index, the faster the pressure reached its final value. This is because a polytropic process with larger polytropic index behaves more like an adiabatic process in which any heat transfer with the surrounding wall is kept to minimum. The compressed air pressure remained constant for the rest of the stroke time due to the fact that the valve has been opened.

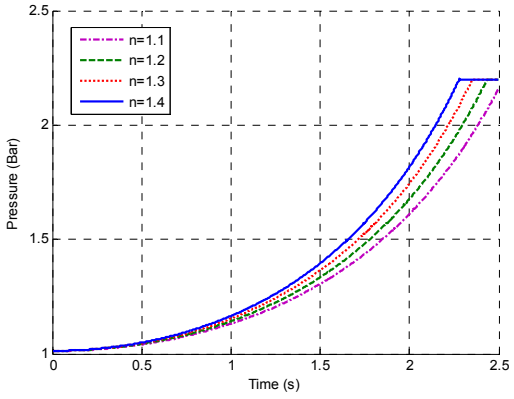

FIGURE 3. PRESSURE VS. STROKE TIME REGARDING TO POLYTROPIC INDEX.

Figure 4 shows the temperature change of the air during the same compression cycle. Similar to the pressure plots, the temperature increased faster and higher with larger polytropic indices. Comparing this data to experimental data will show how well this liquid piston design dissipates heat and maintains the air temperature virtually unchanged, which is significant in preventing heat loss during the process. It is found that the simulated average temperature profile is similar to the analytical case with an index value of between n=1.1 and n=1.2, and as the stroke time is longer, the index values decreases.

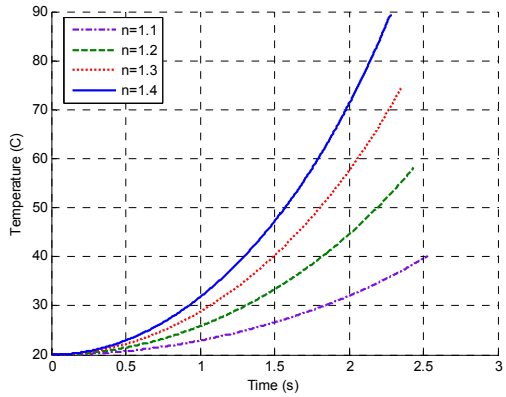

FIGURE 4. TEMPERATURE VS. STROKE TIME REGARDING TO POLYTROPIC INDEX.

EXPERIMENTS FOR PROOF-OF-CONCEPT AND RESULTS

A proof-of-concept tabletop model was built to demonstrate a suitability of integrating a liquid-piston based compression/expansion system into the OCAES system. In the present phase, experiments were performed for compression cycles only, and expansion cycles with an electric generator will be utilized in the future. Initially, a transparent polycarbonate chamber was used in order to visualize the liquid piston movement. This was later replaced by an aluminum alloy chamber which has a higher thermal conductivity needed to realize near-isothermal compression. Temperature and pressure were measured at different stroke speeds.

Experimental setup

The testing experiment for liquid piston prototype is described as a hydraulic circuit shown in Figure 5. This hydraulic circuit consists of four primary components: actuator, liquid piston, storage vessel and hydrostatic tank. Other major components used for the control of compression and storage processes are solenoid valves, pressure regulators, relief valve, micro-control unit (MCU) and relays. Compressed air data is generated by a pressure transducer and a thermocouple. The actuator is designed as two pneumatic cylinders coupled together shown in Figure 6. The purpose of this design is to utilize the existing compressed air source in the laboratory to actuate compression inside the liquid piston. This dual-cylinder actuator is connected to a compressed-air source through a 5/3 solenoid valve and a pressure regulator. The pressure regulator is used to control the 6-bar compressed air coming from the wall source. The 5/3 solenoid valve controls the pressurized and exhausted air flow into and out of the pneumatic cylinder, which determines whether the liquid piston is compressing or retracting. The liquid piston and storage vessel are two identical cylinders in terms of size and material. They are both cut from a length of extruded polycarbonate tube, which provides enough strength for pressure testing up to 3 bars. The two polycarbonate cylinders are pressed fitted into aluminum plates on top and bottom and sealed with rubber O-rings. Water fills the liquid piston, coming in through the bottom aluminum plate.

Another polycarbonate bottle, suspended from the top aluminum plate, serves as a compression chamber into which ambient air is introduced and is placed inside of the liquid piston. In Figure 6, water is dyed light blue to make it easier to visualize the compression chamber in the middle of the liquid piston. Note also that the compression chamber is filled with ambient air, which is transparent in the figure. Two 2/2 solenoid valves are connected to the liquid piston on top. One is open to ambient air for water retraction while the other one is connected to storage vessel. A pressure sensor is connected to the compression chamber so that when the compressed air reaches the desired pressure, the valve opens to let the compressed air out into the storage vessel. A thermocouple is placed at the top and center of the compression chamber, where a maximum transient temperature increase is found to be located in preliminary numerical studies.

The storage vessel on the right of the figure is partially filled with water and connected to a hydrostatic tank at the bottom right. The hydrostatic tank is also connected to a compressed-air source from the wall and regulated to the same pressure as the compressed air in liquid piston. This tank is installed with a bladder inside the tank which separates air and water, which makes it convenient to keep the storage vessel at the simulated hydrostatic pressure. The purpose of this hydrostatic tank is to model the constant hydrostatic pressure at ocean depth, so that the compressed air stored in the storage vessel will be kept at the same pressure during the entire storing phase.

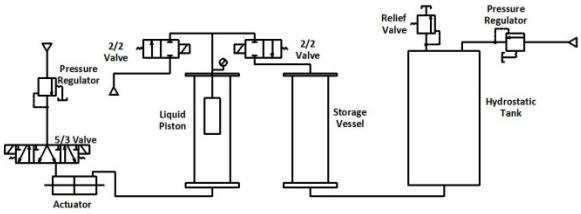

FIGURE 5. HYDRAULIC CIRCUIT FOR LIQUID PISTON PROTOTYPE.

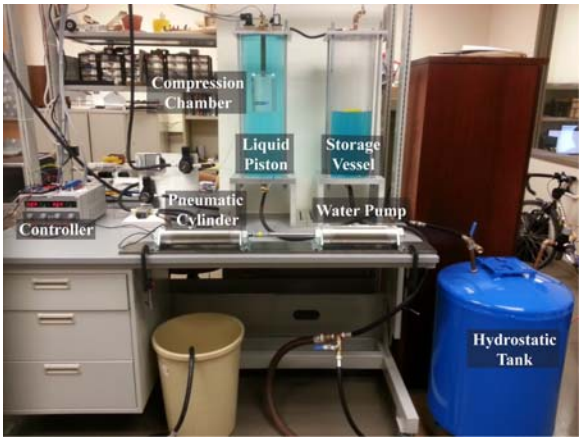

FIGURE 6. PROTOTYPE ASSEMBLY OF THE LIQUID PISTON BASED OCAES SYSTEM.

Experimental Results and Analysis

Initially, a transparent compression chamber is used to observe the interaction between air and water as air is compressed by water or injected from the ambient. The material of the chamber is polycarbonate whose thermal conductivity is between 0.19 ~ 0.22 W/(m·K). Due to the low thermal conductivity, the polycarbonate chamber was intentionally used for demonstration purpose and later is replaced by an aluminum alloy chamber. The thermal conductivity of the alloy is around 170 W/(m·K), which is 850 times higher than that of polycarbonate. Two different materials of the pipe connecting the compression chamber and outer valves were also used as shown in Figure 7, and their dimension is shown in Table 3 previously.

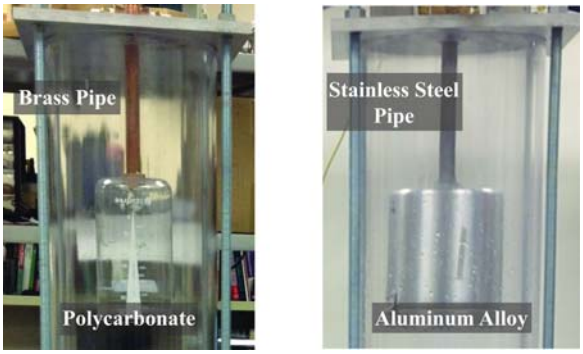

FIGURE 7. COMPRESSION CHAMBER WITH DIFFERENT MATERIALS.

The experiments were performed at six different stroke times; 2.5 5 10 15 20 and 40 seconds, and temperature of air in the chamber is measured at 100 Hz sampling frequency. A very fine gage thermocouple whose diameter is 0.001 inches was placed at the top of the compression chamber, and effort was made to make sure that it does not come in contact with the pipe or the chamber. The pressure was measured at 60 Hz sampling frequency at the end of the pipe. The compression ratio was set to 2.21:1. Air temperature for the adiabatic compression was calculated by $T_2 = T_1(P_2/P_1)^{(\gamma-1)/\gamma}$ where T_1 is 296.53 °K, where γ is 1.4 for ideal gas. The maximum temperature for the adiabatic compression is calculated to be at 371.93 °K, which indicates a temperature increase of 98.8 °C. The measured temperature from the actual table-top system, therefore, is expected to fall between ambient and this maximum temperature.

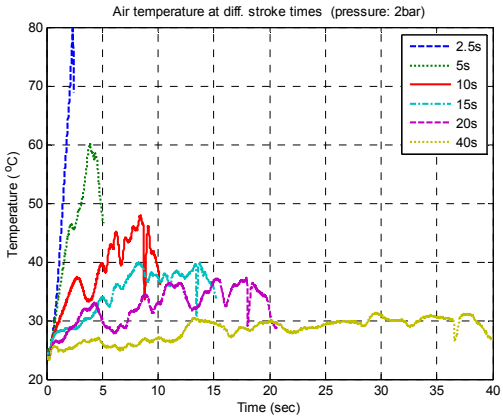

FIGURE 8. AIR TEMPERATURES OF THE ALUMINUM PISTON AT DIFFERENT STROKE TIMES.

The air temperature measurements for six different stroke times are shown in Figure 8. It was observed that the temperature increments reduced as the stroke time was increased. For the 2.5-second stroke, the temperature increment reaches 80 degrees which is almost the adiabatic temperature. However, the maximum air temperature decreases as the stroke time gets longer, and for the 40-second stroke, the temperature increases within 6~7 degrees. The average temperature will be much smaller than the local temperature.

The simulations were conducted for finding the average temperature. ANSYS CFX was used for a single stroke compression simulation. Two phases, which are air and water, and transient simulation at 2.5 second stroke time was chosen. The final desired pressure was set as 2.21 bars, and when the air pressure reached the final pressure, the exhaust valve was opened in order

to transport the compressed air into the storage. The time step was chosen as 0.001 seconds which results 2,500 total time steps.

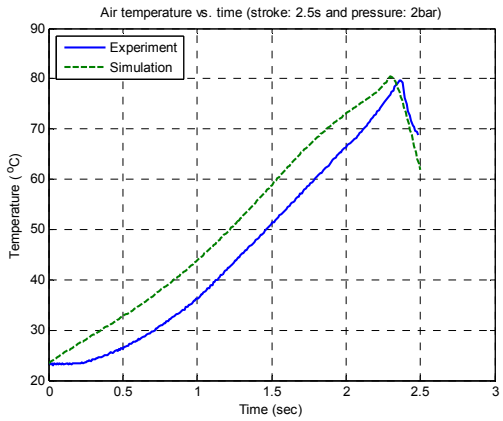

(A) AIR TEMPERATURE

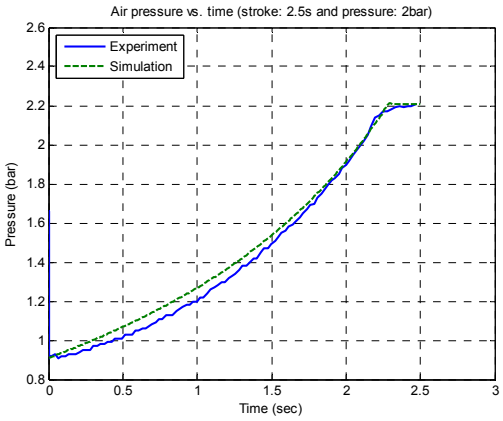

(B) AIR PRESSURE

FIGURE 9. COMPARISON BETWEEN EXPERIMENT AND SIMULATION RESULTS.

Figure 9 shows the comparison between experiment and simulation results. The simulation temperature was calculated at the similar location as the experiment where the thermocouple was installed. This spot is hottest because it is the center of the final volume of compressed air. As shown, both experiment and simulation temperature reached around 80 degrees when the air was compressed at 2.21 bars. The temperature profile predicted by the simulations does not exactly match the experimental results as seen in Figure 9. The reason for this can be attributed to thermal inertia of the air. The experimental temperature measurements show that the slope of temperature rise is low initially and increases by about 0.5 second. Following this the slopes of both the simulation results and experimental measurements are identical. On the other hand, the pressure lines are similar because generally local pressure is not very different from the averaged pressure, and pressure transfers very fast at speed of sound. This implies that the simulation can be used to calculate average temperature values which are hard to measure in experimental setups.

The average temperature was calculated using volume integration with air volume fraction at each time step as shown in Figure 10. The maximum average temperature was 48.6 degree Celsius which is almost half compared to the local point temperature. If the stroke time is longer, the averaged air temperature would be lower.

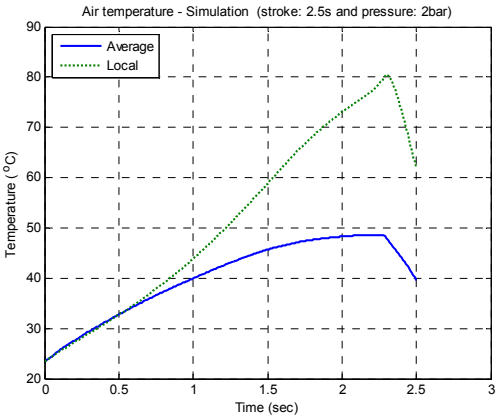

FIGURE 10. AVERAGE AND POINT TEMPERATURE OF SIMULATION.

CONCLUSIONS

In this paper, an analysis and a proof-of-concept experiment of a compression process for the OCAES system were conducted. A liquid-piston based compression cycle was proposed for high energy efficiency. For the heat transfer analysis, a simple single-cylinder-type piston was modeled and analyzed based on convective heat transfer and a fully developed internal fluid flow. Transient numerical results of this model were obtained from a polytropic compression with several polytropic index values for 2.5-second stroke.

An important contribution of the paper was building and testing a table-top liquid-piston and air-storage model that emulates the OCAES concept. The proof-of-concept experiment of a liquid piston coupled to an OCAES system was tested and preliminary data measured and analyzed. Six different stroke times were used to conduct experiments at compression ratio 2.2:1. The minimal temperature increments were observed as the stroke time increased, which proved a near-isothermal nature of the liquid piston process. From the simulations, it suggested that a slight expansion of dead volume during water retraction can mitigate the temperature increase and keep the overall process near-

isothermal. This kind of mitigating technique would be crucial for actual implementation of a larger system with more chambers. In addition, the location of the temperature sensor used in the liquid piston needs further investigation to verify the average temperature from the simulations. Stroke profile, which also involves stroke displacement and frequency, needs further optimization to realize even closer isothermal process. Finally, an optimization of physical size and shape of the compression chamber will result in increasing the heat transfer rate [17].

In summary, the liquid piston concept promises noteworthy efficiency enhancements and many future applications for renewable energy storage systems, as well as for conventional compressor/expander systems. The proof-of-concept experiment performed here will be used as a guide to develop a scaled-up design and implementation of an OCAES system in future.

ACKNOWLEDGEMENTS

The authors gratefully acknowledge the funding from the North Carolina Coastal Studies Institute for the work described in the paper.

REFERENCES

[1] Gatzen, C., 2008, *The Economics of Power Storage: Theory and Empirical Analysis for Central Europe*, Oldenbourg Industrieverlag, Munich, Germany.

[2] Ter-Gazarian, A., 1994, *Energy Storage for Power Systems*, IEE Energy Series 6, Peter Peregrinus Ltd., Herts, UK.

[3] Seymour R. J., 1997, "Undersea Pumped Storage for Load Leveling," *Proceedings of the California and the World Ocean '97*, ASCE, San Diego, pp. 158-63.

[4] Seymour, R. J., 2007, "Ocean Energy On-demand Using Underocean Compressed Air Storage," *Proceedings of the 26th International Conference on Offshore Mechanics and Arctic Engineering*, ASME, San Diego, pp. 527-31.

[5] Lim, S. D., Mazzoleni, A. P., Park, J. K., Ro, P. I., and Quinlan, B., 2013, "Conceptual Design of Ocean Compressed Air Energy Storage System," MTS Journal, **47**(2), pp. 70-81.

[6] Ingersoll, E. D., Aborn, J. A., and Chomyszak, S. M., 2012 "Compressor and/or Expander Device," United States patent US 8096117B2.

[7] Bollinger, B. R., 2010, "System and method for rapid isothermal gas expansion and compression for energy storage," United States patent US 7802426.

[8] Fong, D. A., Crane, S. E., and Berlin, Jr. E. P., 2012, "Compressed Air Energy Storage System Utilizing Two-phase Flow to Facilitate Heat Exchange," United States patent US 8182240.

[9] Converse, A. O., 2012, "Seasonal Energy Storage in a Renewable Energy System," Proceedings of the IEEE, **100**(2), pp. 401-9.

[10] Van de Ven, J. D., and Li, P. Y., 2009, "Liquid piston gas compression," Applied Energy, **86**(10), pp. 2183-91.

[11] Holman, J. P., 2002, *Heat transfer*, McGraw-Hill Inc., New York.

[12] Smits, A. J., and Dussauge, J., 2006, *Turbulent shear layers in supersonic flow*, Springer Science+Business Media Inc., New York.

[13] Crane Co., 1988, *Flow of fluids through valves, fittings, and pipe*, Technical Paper (TP 410).

[14] Weast, R. C., Astle, M. J., and Beyer, W. H., eds., 1984, *CRC handbook of chemistry and physics*, CRC Press Inc., Boca Raton, FL.

[15] Kays, W. M., and Crawford M. E., 1993, *Convective heat and mass transfer*, McGraw-Hill, New York.

[16] Incropera, F. P., Dewitt, D. P., Bergman, T. L., and Lavine, A. S., 2007, *Fundamentals of heat and mass transfer*, John Wiley & Sons, New York.

[17] Saadat, M., Li, P. Y., and Simon, T., 2012, "Optimal Trajectories for a Liquid Piston Compressor/Expander in a Compressed Air Energy Storage System with Consideration of Heat Transfer and Friction," *Proceedings of the 2012 American Control Conference*, Montreal, Canada, pp. 1800-05.